J. Phys. B: Atom. Molec. Phys., Vol. 12, No. 1, 1979. Printed in Great Britain

Electron impact excitation of $1^1S \rightarrow 2^1P$ and $1^1S \rightarrow 3^1P$ of helium: excitation cross sections and polarisation fractions obtained from XUV radiation

W B Westerveld, H G M Heideman and J van Eck

Fysisch Laboratorium Rijksuniversiteit, Princetonplein 5, 3508 TA Utrecht, The Netherlands

Received 16 June 1978

Abstract. The excitation of the 2^1P and 3^1P states of helium by electrons has been studied in the energy range from near threshold to 2 keV. This was done by observing the XUV radiation produced at emission angles of 55° and 90° to the incident electron beam. Fano plots of the relative data were fitted by straight lines in the high-energy region. The measurements were brought on an absolute scale by normalising the 'relative' slopes of the fits to the slopes predicted by the Bethe approximation. Special attention has been paid to systematic errors introduced by the use of a blazed concave grating. For energies exceeding 350 eV the total cross sections are in agreement with the Bethe approximation. In the lower energy region (30–300 eV) the total cross sections are in good agreement with recent distorted-wave calculations. By combining the results obtained at 55° and at 90° to the electron beam, total cross sections for excitation of the magnetic sublevels were obtained. The optically forbidden character of the $m = 0$ sublevel excitation becomes manifest for electron energies exceeding 500 eV. Polarisation fractions were derived from the experimental results in the energy range 30–300 eV.

1. Introduction

In the past accurate total cross sections have been obtained for excitation of helium to the 2^1P and 3^1P levels by electron impact at energies from near threshold up to several keV (de Jongh and van Eck 1971, Donaldson *et al* 1972). The determination of total cross sections over such a large energy range is carried out by firing an electron beam of well defined energy through the gas under study. Usually the intensity of the radiation (originating from the decay of atoms excited to the level concerned) emitted at well defined angles with respect to the incoming electron beam is then recorded as a function of the electron energy. In general the recorded intensities have to be corrected, both for polarisation effects and for effects of cascade from higher lying levels, before cross sections for the direct process of excitation by electrons can be derived. Depending on the wavelength of the observed transition, the conversion of the relative intensity data to an absolute scale may impose difficulties. In the studies referred to above, this normalisation has been performed in a semi-theoretical way by means of the well known Bethe approximation (Inokuti 1971).

In the present work, just as in the two papers mentioned above a vacuum-ultraviolet spectrometer has been used to observe the intensity of the transitions from the 2^1P and

0022-3700/79/010115+21$01.00

3^1P states to the ground state. The range of electron energies used extends from threshold to 2 keV.

Our intention is:

(i) to provide more data on the *absolute* excitation cross sections in the range of lower electron energies. This seems of some importance because of the theoretical efforts which have recently been undertaken in that energy range following the advent of electron–photon coincidence experiments (Eminyan *et al* 1974).

(ii) to determine, with more emphasis on experimental errors than has been done previously, the region of validity of the Bethe approximation in predicting total excitation cross sections.

(iii) to combine measurements on the intensity of radiation emitted at different angles to the incoming electron beam to obtain total cross sections for excitation of sublevels or (equivalently) to obtain polarisation fractions.

2. Experimental

The apparatus used in the present investigation has been described elsewhere (Westerveld and van Eck 1977). In short the gas under study is admitted to a vacuum chamber in which an electron beam system is placed. The electron beam system consists of an electron gun with Pierce extraction system, a scattering cell and a Faraday cup. The vacuum chamber is connected to the entrance slit of a separately pumped VUV spectrometer with a concave grating as the dispersive and imaging element (used in near-normal incidence). The concave grating (radius 1 m; 1200 lines/mm) can be moved along the Rowland circle for wavelength selection; the entrance and exit slits are at a fixed position on the Rowland circle. Ultraviolet photons resulting from the excitation of gas atoms have to travel about 8 cm before reaching the entrance slit of the spectrometer. After dispersion the intensity of radiation of the selected wavelength is detected at the exit slit with the help of an electron multiplier.

The electron gun is placed at such angles that the plane formed by the electron beam and the observed direction of photon emission is at 45° to the entrance slit of the spectrometer. In this way the sensitivity of the dispersive element for the polarisation of the incoming radiation from the beam-excited atoms is largely eliminated (see Clout and Heddle 1969). The venetian-blind-type multiplier which we used (EMI 9642) was oriented in such a way that the linear cathode structure was at right angles to the exit slit of the spectrometer. For reasons of symmetry no polarisation effects from the multiplier are to be expected when the electron beam system is oriented in the above described way.

We deliberately chose an arrangement in which the whole electron gun is immersed in the gas and not a crossed beam set-up as used by Donaldson *et al* (1972). In an apparatus with crossed beams it is difficult to avoid changes in the cross sectional area of the electron beam when the energy is changed so that the collision rate may be influenced. On the other hand, our arrangement necessitates the use of very low helium pressures to avoid absorption of the resonance photons by the surrounding gas. The disturbing effect here is not the absorption itself (because the ground-state atoms absorbing the radiation are isotropic) but rather the re-emission after absorption. The re-emission changes the intensity distribution over the emission angles. In the present work we used pressures of 2×10^{-4} Pa ($\simeq 1{\cdot}5\times10^{-6}$ Torr) and 8×10^{-4} Pa ($\simeq 6\times 10^{-6}$ Torr) for the transitions $2^1P\rightarrow 1^1S$ and $3^1P\rightarrow 1^1S$, respectively. As may be seen

from a plot of transmission against pressure (figure 1) for the radiation from the transition $2^1P \rightarrow 1^1S$, less than 10% of the resonance photons are absorbed at this pressure. In a previous paper (Westerveld and van Eck 1977) we have shown that at the above pressures no significant contribution of re-emission from atoms excited by absorption of resonance photons was present. The pressures used are also sufficiently low that processes due to collisions between excited- and ground-state atoms can be neglected.

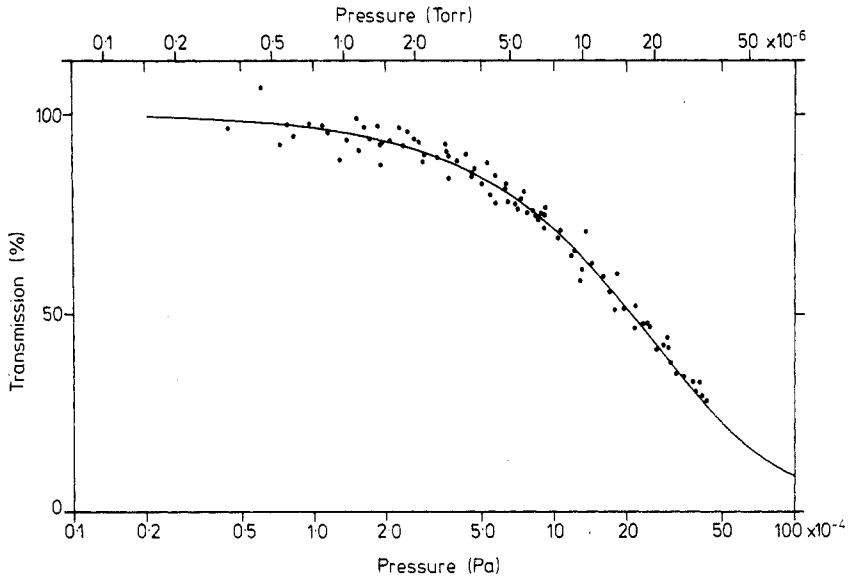

Figure 1. Transmission of $He(2^1P \rightarrow 1^1S)$ resonance radiation through the target gas as a function of pressure (measured at room temperature over an absorption length of about 8 cm). The points represent intensities divided by the pressure as obtained from experiment. The data were normalised by imposing the condition that extrapolation to zero pressure should give a transmission of 100%. The full curve gives the theoretical transmission calculated for a purely Doppler-broadened line using an absorption oscillator strength $f_2 = 0{\cdot}262$ (for more details see Westerveld and van Eck 1977).

In the experiments the electron beam currents ranged from 100–150 μA in the region of higher electron energies ($\gtrsim 250$ eV) to less than 20 μA in the lower energy region. Emission of photons was observed at two different angles θ with respect to the electron beam; namely $\theta \simeq 55°$ ('magic angle', $\cos^2\theta = \frac{1}{3}$) and $\theta \simeq 90°$.

At each selected electron beam energy E measurements were performed by integrating during a certain time the electron beam current with the help of a Coulomb integrator and counting the pulses from the multiplier. Relative emission cross sections were obtained by correcting the accumulated number of counts for the average number of the background counts and by dividing by the accumulated electronic charge transmitted through the scattering cell, and by the helium pressure. At each of the two observed emission angles about five measuring series were obtained, separately for the high-energy region (100–2000 eV) and the low-energy region (25–100 eV). After averaging the different series, RMS errors could be assigned to the mean values of the relative emission cross sections ($S_m(E)$ and $S_\perp(E)$ for observation at $\theta \simeq 55°$ and 90° to

the electron beam, respectively). In this way all errors of a statistical nature (such as uncertainty due to the finite number of counts and small pressure variations) are taken into account. In the high-energy region ($E \geqslant 100$ eV) the RMS errors obtained were of the order of 1%. The background count rate of the multiplier was always smaller than one count per ten seconds†. For measurements in the high-energy region, the background count rate never exceeded a few per cent of the signal count rate. Systematic errors arise when a fraction of the excitation is due to secondary electrons produced by primary electrons hitting metal surfaces or by reflection of primary electrons. In the high-energy region this sort of error could be eliminated for the greater part by choosing suitable potentials in the electron gun. In the low-energy region ($E \leqslant 150$ eV) this was more difficult to do. The reason was that the current passing through the scattering cell could not be collected in total; a correction was applied by measuring the current separately on the backplate of the scattering cell. The maximum current drawn by the backplate was of the order of 5% of the total current at low voltages.

The energy definition of the electron beam was checked by measuring the near-threshold part of the excitation function of the 2^1P state. The well known resonance feature at 22·6 eV (Chamberlain and Heideman 1965, Brunt *et al* 1977) served as a calibration point (see figure 2). An energy shift of about 1·6 eV was found with respect to the applied voltage. This shift was taken into account in the choice of voltage differences between the cathode and scattering cell, in order to get round numbers for the energies at which the cross sections were determined. In the low-energy region, where there is a strong variation of the excitation cross section with electron energy, the inaccuracy in the electron energy is reflected in an increase of the error in the excitation

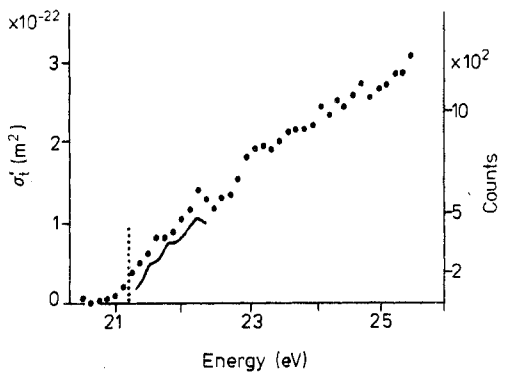

Figure 2. Threshold part of the excitation function $1^1S \rightarrow 2^1P$ of helium (not corrected for cascade) as obtained at an emission angle of 55° to the exciting electron beam. The resonance feature at 22·6 eV served as a calibration point for the energy scale. Normalisation of the cross section was performed by comparing the count rate at 25 eV with the count rate at higher energies (100–250 eV). The actual numbers of counts as displayed at the right hand side of the figure are displaced by forty counts to account for the number of background counts. The full curve represents the calculation of Oberoi and Nesbet (1973).

† In the course of this investigation we found even low-energy electrons capable of producing quite intensive background radiation when metal surfaces in view of the spectrometer were subjected to electron bombardment. This phenomenon (which does not play a role in the present experiment) seems to be very poorly investigated. As far as the VUV region is concerned the only report we are aware of is that by Lukirskii and Fomichev (1965). Besides bremsstrahlung, transition radiation may also play a role in these phenomena (see Tomaš *et al* 1974).

cross sections obtained at the given energies. We estimate the accuracy of the energy definition to be better than 1 eV. The energy spread in the electron beam is about 0·25 eV FWHM.

3. Anisotropy and polarisation of the emitted radiation

In the case of dipole radiation emitted by atoms excited by an unidirectional electron beam of energy E we have, in general, a non-uniform intensity distribution over the emission angles. In this section we will outline the connection between the intensity distribution of the observed radiation and the parameters describing the electron–atom scattering process leading to the excited state concerned. We will do this somewhat more extensively than is usual in work dealing with total excitation cross sections because of the explicit use of some of the formulae in § 6.

The most direct and general approach to describe the connection between observed photon emission and the excitation cross sections involved is to use the formalism of Macek and Jaecks (1971). Their formulae give the intensity distribution of polarised radiation emitted by atoms excited in a scattering process with well defined collision dynamics (i.e. with specification of the scattering angle of the exciting electron). In the notation of Macek and Jaecks (1971) we get (after integration over all electron scattering angles) for the polarised radiation intensity emitted at an angle θ to the incoming electron beam:

$$\mathcal{I}(E;\theta,\beta) \sim A_{00}\cos^2\beta\sin^2\theta + A_{11}(\sin^2\beta + \cos^2\beta\cos^2\theta). \tag{1}$$

The angle β is the angle between the principal axis of the linear polariser and the plane formed by the electron beam and the observed direction of photon emission (see figure 3). The parameters A_{00} and A_{11} involve (in general) linear combinations of the population densities of the sublevels of the upper state, including their possible time behaviour†. In the present case we work under steady-state conditions, so that the ratio

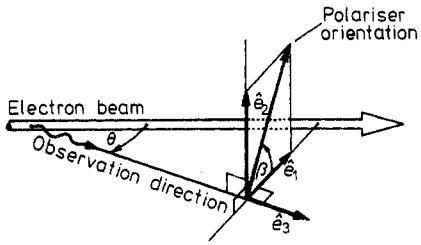

Figure 3. Definition of the system of reference axes $\{\hat{e}_1, \hat{e}_2, \hat{e}_3\}$ connected to the direction of observation to describe the orientation of a linear polariser. The axis $\hat{e}_3$ is chosen along the direction of observation; $\hat{e}_2$ is taken perpendicular to $\hat{e}_3$ and to the electron beam and $\hat{e}_1$ is perpendicular to both $\hat{e}_2$ and $\hat{e}_3$.

† Equation (1) suggests that the source of radiation consists of three *independent* classical dipole oscillators: one along the electron beam direction and two perpendicular to each other and to the electron beam (one of which is in the plane formed by the electron beam and the direction of observation). It is clear then that the principal axes of polarisation are along $\hat{e}_1$ and $\hat{e}_2$, respectively (figure 3), as may also be seen directly from symmetry arguments. This immediately suggests the orientation of the electron beam in such a way that the plane formed by $\hat{e}_1$ and $\hat{e}_3$ is at an angle of 45° with the entrance slit of the spectrometer, to overcome the sensitivity of the apparatus for the polarisation degree of the radiation (see § 2).

of A_{00} and A_{11} is expressible in terms of the sublevel excitation cross sections. For a transition $n^1\mathrm{P} \rightarrow 1^1\mathrm{S}$ in helium (LS coupling) we have:

$$\mathcal{J}(E;\theta,\beta) \sim \sigma_0'(E)\cos^2\beta\sin^2\theta + \sigma_{\pm1}'(E)(\sin^2\beta + \cos^2\beta\cos^2\theta) \tag{2}$$

where $\sigma_0'(E)$ and $\sigma_{\pm1}'(E)$ are the cross sections for excitation of the magnetic sublevels with $m = 0$ and $m = \pm 1$, respectively. Here and in the following we use primed symbols to indicate that contributions by processes of cascade from higher lying levels are *included*. The spatial symmetries of the scattering process imply $\sigma_{-1}' = \sigma_{+1}'$. (The scattering process is invariant for reflection with respect to an arbitrary plane containing the electron beam.) The direction of the incoming electron beam is chosen as the axis of quantisation. With the usual definition for the polarisation fraction $\Pi'(E)$ we find:

$$\Pi'(E) = \frac{\sigma_0'(E) - \sigma_{\pm1}'(E)}{\sigma_0'(E) + \sigma_{\pm1}'(E)} \tag{3}$$

and consequently:

$$I(E;\theta) = \frac{3}{4\pi} I_t(E) \frac{1 - \Pi'(E)\cos^2\theta}{3 - \Pi'(E)} \tag{4}$$

where $I(E;\theta)$ is the intensity of radiation summed over two mutually perpendicular polariser settings, emitted at an angle θ with the incoming electron beam and $I_t(E)$ is the total intensity (integrated over all emission angles). Generally defining the polarisation degree $P'(E;\theta)$ of the radiation observed at an emission angle θ to the electron beam as:

$$P'(E;\theta) = \frac{\mathcal{J}(E;\theta,\beta=0) - \mathcal{J}(E;\theta,\beta=\pi/2)}{\mathcal{J}(E;\theta,\beta=0) + \mathcal{J}(E;\theta,\beta=\pi/2)} \tag{5}$$

we find

$$P'(E;\theta) = \frac{\Pi'(E)\sin^2\theta}{1 - \Pi'(E)\cos^2\theta}. \tag{6}$$

Only for $\theta = \pi/2$ do we have $P' = \Pi'$ but, in general, we get $|P'| \leqslant |\Pi'|$.

4. Evaluation of cross sections: normalisation procedure

For the total intensity emitted in the transition considered we have (by definition):

$$I_t(E) = \gamma\sigma_t'(E) n l i / e \tag{7}$$

with γ the branching ratio of the observed transition, n the number density of the ground-state helium atoms, i the electron beam current, e the electronic charge, l the length of the observed part of the beam and $\sigma_t'(E)$ the total cross section (summed over the magnetic sublevels) for excitation of the observed level from the ground state. In the present case we have

$$\sigma_t'(E) = \sigma_0'(E) + 2\sigma_{\pm1}'(E). \tag{8}$$

For the detected count rate we write down

$$R(E;\theta_0) = \eta \int_{\Omega_0} I(E;\theta)\,\mathrm{d}\Omega \tag{9}$$

with η the overall quantum efficiency of the spectrometer and the detector. The integration is performed over the solid angle Ω_0 defined by the aperture of the spectrometer and centred around an angle of emission θ_0 with the electron beam. For the relative emission cross sections $S(E;\theta)$ as introduced in § 2 we thus have:

$$S(E;\theta) \sim \sigma_0'(E)\sin^2\theta + \sigma_{\pm 1}'(E)(1+\cos^2\theta) \tag{10}$$

provided that both Ω_0 and l are sufficiently small (see § 6).

4.1. Measurements at 55° with the electron beam

Although in principle it is possible to obtain experimentally absolute values of η for vacuum-ultraviolet lines (e.g. Mentall and Morgan 1976) we will use the semi-theoretical normalisation method via the Bethe approximation. In the papers of, for example, de Jongh and van Eck (1971) and Donaldson *et al* (1972) the functional energy dependence of the total cross section in the Bethe approximation was used to normalise their relative data obtained at emission angles of about 55° to the exciting electron beam. At this emission angle the data are directly proportional to the total excitation cross section $\sigma_t'(E)$ (cf equations (3), (4) and (8)). The Bethe approximation gives the asymptotic behaviour of the Born approximation in the high-energy region. For the transitions studied here, we have in the Bethe approximation (for a review see Inokuti 1971)

$$\sigma_t(E) = \frac{4\pi a_0^2}{E/R}\frac{f_n}{E_n/R}\ln(4c_nE/R) \tag{11}$$

where a_0 is the first Bohr radius of hydrogen, R the Rydberg energy, E_n the excitation energy and f_n the optical oscillator strength of the transition from the ground state to the level considered and finally c_n is a dimensionless constant related to the shape of the generalised oscillator strength as a function of the momentum transferred in the collision. A plot of the product $\sigma_t(E)E$ against $\ln(E/R)$ (the so called Fano plot) should result in a straight line with slope $4\pi a_0^2R^2f_n/E_n$.

In the high-energy region ($E \geqslant 100$ eV) we corrected the relative emission cross sections $S_m(E)$ for cascade by using published values for the cascade contributions (de Jongh 1971, Donaldson *et al* 1972). These corrections are small (see § 7.1). The corrected values of $S_m(E)$ were plotted in a Fano plot and weighted straight-line fits were made to the points. As weights we used the inverted and squared RMS errors (see for instance Mathews and Walker 1970) as obtained from the experiment (see § 2). In this way it is possible to carry out a χ^2 test on the quality of the fit. By dropping successively in each new fit a measurement on the low-energy side of the fit, it may be decided at which energy straight-line behaviour fits within the accuracy of the experiment. The lowest (normalised) χ^2 values so obtained were smaller than one ($\simeq 0{\cdot}4$). A possible reason may be small differences in the quantum efficiency of the apparatus for the different measuring series; this would result in an overestimation of the RMS errors in the *relative* values $S_m(E)$. The plots obtained are given in figure 4. We will now follow the procedure as described by van Eck and de Jongh (1970). The 'relative' slope obtained from the fits is normalised to the slope according to the Bethe approximation (equation (11)). (Accurate values for the oscillator strengths of the transitions considered are available, see e.g. Schiff *et al* (1971) and § 7.1.) The normalisation factor which is found is used in the conversion of the relative data to

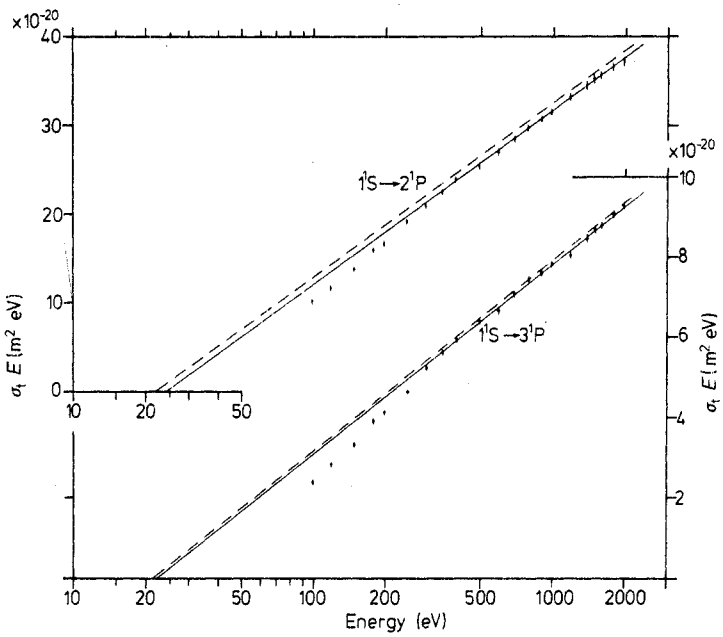

Figure 4. Fano plots of the total excitation cross sections $\sigma_t = \sigma_0 + 2\sigma_{\pm 1}$ (corrected for cascade) for the transitions $1^1P \rightarrow 2^1P$ and $1^1S \rightarrow 3^1P$. Points: experimental values obtained at an emission angle of 55° to the incident electron beam. The error bars represent the statistical errors as obtained from the experiment. The measurements were brought on an absolute scale by normalisation to the slope of the Fano plot in the Bethe approximation (see § 4.1). The full lines give the weighted least-squares fits to the plotted points in the energy range from 350 to 2000 eV. The intersections of these fits with the energy axis are at 24·6 and 22·1 eV for excitation of the 2^1P and 3^1P levels, respectively. The broken lines, representing the Bethe approximation as obtained from the calculations of Kim and Inokuti (1968), intersect the energy axis at 22·7 and 21·20 eV, respectively.

absolute excitation cross sections. The correctness of the calibration method as outlined, remains to be verified especially with regard to the slope of the Fano plot as predicted by the Bethe approximation (see § 5).

4.2. Measurements at 90° with the electron beam

To bring the data obtained at right angles to the electron beam on an absolute scale equation (11) cannot be used. The relative emission cross sections $S_\perp(E)$ are proportional to the sum $\sigma_0'(E) + \sigma_{\pm 1}'(E)$ and in general not to the total cross section $\sigma_t'(E)$. Some years ago a Bethe theory was worked out for polarisation by McFarlane (1974). Application of his formula to the present case yields the following Bethe asymptotic cross sections for excitation of the sublevels:

$$\sigma_0(E) = \frac{4\pi a_0^2}{E/R} \frac{f_n}{E_n/R} \tag{12}$$

$$\sigma_{\pm 1}(E) = \frac{2\pi a_0^2}{E/R} \frac{f_n}{E_n/R} [\ln(4c_n E/R) - 1]. \tag{13}$$

The functional relationships between the cross sections for excitation of the

sublevels and the electron energy had been noticed previously by Moustafa Moussa (1967). Writing $\sigma_\perp(E) = \sigma_0(E) + \sigma_{\pm 1}(E)$ we find:

$$\sigma_\perp(E) = \frac{2\pi a_0^2}{E/R} \frac{f_n}{E_n/R} \ln(4 d_n E/R) \tag{14}$$

with

$$\ln d_n = \ln c_n + 1. \tag{15}$$

The normalisation of data at right angles may now be carried out (at least in principle) with the help of a Fano plot via equation (14).

Cascade corrections were applied under the assumption that the cascade contributions were unpolarised. This is not entirely correct (radiation from the ^{1}D levels may be polarised) but the cascade corrections are small and do not influence the shape of the relative emission cross sections in a significant way. However, when we tried to treat the data obtained at right angles to the electron beam along the lines sketched in § 4.1, it appeared that the asymptotic straight-line behaviour according to the Bethe approximation was not reached until much higher energies than in the case of the total cross sections. This resulted in poorly defined fits and consequently a poorly defined normalisation.

Therefore a different approach was adopted to normalise the data obtained at right angles to the electron beam. The $\ln c_n$ values acquired from the fits to the Fano plots for the 2^1P and 3^1P total excitation cross sections were used to find the values $\ln d_n$ via equation (15). From these $\ln d_n$ values the energies are found (equation (14)) where the fits to the Fano plots of the data obtained at right angles to the electron beam should intersect the energy axis (see figure 5). The fits were made through this intersection and the plotted points with $E \geqslant 1000$ eV (the fit did not change when a few points on the low energy side were added). Figure 5 was brought on an absolute scale by comparing the 'relative' slopes of the plots obtained in the above way with the theoretical slope $2\pi a_0^2 R^2 f_n/E_n$ of the Bethe approximation (equation (14)). In this way absolute excitation cross sections $\sigma'_\perp(E)$ are acquired. By combining the results obtained at emission angles of 90° with those obtained at 55°, separate excitation cross sections are acquired for the sublevels. Because the combination of these measurements involves a subtraction, the statistical errors are enlarged. This may also be the case for systematic errors (especially for $E \leqslant 150$ eV) which may be of importance in our case because a shorter scattering cell of different geometry was used for measurements at right angles to the electron beam. In view of this difficulty we have to be cautious in drawing conclusions (§ 7.2).

5. Justification of the normalisation procedure

A first check whether or not the Bethe asymptotic cross section is actually reached in the experiment may be carried out by comparing the $\ln c_n$ values obtained from the Fano plots with the accurate calculations of Kim and Inokuti (1968) (see also table 1 and § 7). However, the important parameter in the normalisation procedure of the present *relative* measurements is the slope $4\pi a_0^2 R^2 f_n/E_n$ of the Fano plot as given in the Bethe approximation. The only possible way to prove the correctness of the Bethe approximation in predicting the slope is to perform in some way an absolute measurement of the total cross section. For the 3^1P level this is possible by observing the transition

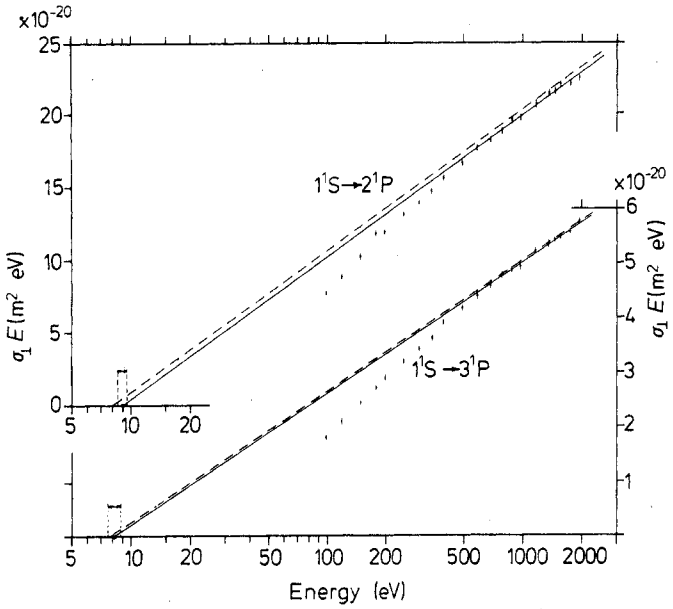

Figure 5. Fano plots of the excitation cross sections $\sigma_\perp = \sigma_0 + \sigma_{\pm 1}$ (corrected for cascade) for the transitions $1^1S \rightarrow 2^1P$ and $1^1S \rightarrow 3^1P$. Points: experimental values obtained at right angles to the incident electron beam. The error bars represent the statistical errors as obtained from the experiment. The measurements were brought on to an absolute scale by normalisation to the slope of the Fano plot in the Bethe approximation (see § 4.2). The full lines give the fits made through the plotted points with $E \geq 1000$ eV and through the points at 9·0 eV and 8·1 eV on the energy scale for excitation of the 2^1P and 3^1P, respectively. The points at 9·0 and 8·1 eV with their error limits (↔) were derived from the results of the measurements at 55° to the electron beam (figure 4) using equations (14) and (15). The broken lines represent the Bethe approximation as obtained from the calculations of Kim and Inokuti (1968).

$3^1P \rightarrow 2^1S$. The branching ratio of this transition is known and in the visible region of the spectrum absolute calibration of the equipment is possible by standard optical means (van Raan *et al* 1971, Showalter and Kay 1975). Within the rather large error limits ($\simeq 10\%$) of this type of calibration the Bethe asymptotic cross section for excitation of the 3^1P state is reached at electron energies of a few hundred eV. For excitation of the 2^1P level rigorous tests have been performed by integration of differential cross sections obtained in electron scattering experiments (Vriens *et al* 1968, Dillon and Lassettre 1975). It was shown (Dillon and Lassettre 1975) that from 300 eV onwards, fitting of apparent generalised oscillator strengths to an adapted polynomial and numerical integration leads to total cross sections within 3% of the Bethe values (see also table 2). So the use of the Bethe normalisation procedure for total cross sections as outlined in § 4 appears to be justified for the transitions considered here.

6. Some sources of systematical error (of geometrical origin)

In writing down equation (10), several assumptions were made:

(A) It was assumed that the variation of θ along the observed part of the beam is sufficiently small to allow the rewriting of equation (9) into (10). In the present case the

variation of θ is of the order of $\pm 2°$. The systematic error introduced by the use of equation (10) remains smaller than 0·1%, provided that there is no variation in efficiency over the aperture of the spectrometer.

(B) It was assumed that the electron gun is oriented in such a way that the quantum efficiency η of the apparatus is independent of the degree of polarisation of the observed radiation (see equation (9)). Except for the case when the electron gun is parallel to the surface of the grating this condition cannot be realised for each part of the grating at the same time. Just as in (A) the systematical error introduced by the use of equation (10) will be negligibly small only when there is no variation in efficiency over the aperture of the spectrometer.

However the use of a *blazed concave* grating in the spectrometer may give rise to errors, caused by the strong variation of the efficiency over the grating (Samson 1967, Hunter 1974). The blaze wavelength of the grating we used is given as 120 nm, but in fact this value is only correct for the central part of the grating because the local blaze angle changes from one side of the grating to the other. By partly screening the grating, it was found that only the extreme left part of the grating was effective when the helium lines were observed in first order. In second order a much larger part of the grating was effectively used. (The measurements were carried out therefore in second order). The result of the unknown variation of the efficiency over the surface of the grating may be that the effective acceptance solid angle of the spectrometer is no longer exactly centred around the supposed direction with respect to the electron beam (55° or 90°). As a consequence two types of error will be present:

(A′) The average angle θ with the electron beam at which the observed radiation is emitted deviates somewhat from the supposed value (55° or 90°). Therefore the relationship between $I(E; \theta)$ on the one hand and $I_t(E)$ and $\Pi'(E)$ on the other is not used correctly (see equation (4)).

(B′) The quantum efficiency η of the apparatus is no longer fully independent of the degree of polarisation of the observed radiation. For observation at 55° to the electron beam these effects are more pronounced than in the case of observation perpendicular to the electron beam because the spectrometer was used in near-normal incidence (although the polarisation degree of the radiation is higher for observation at right angles to the electron beam, see equation (6)). At the multiplier we once more have an incomplete elimination of the difference in efficiency for detection of radiation with electric vector parallel or perpendicular to the exit slit (the linear cathode structure of the multiplier was oriented at right angles to the exit slit). This would also be the case when a channeltron detector was used, because, on average, the incident radiation is not necessarily incident along the axis of the channeltron. The use of a tripartite ruled grating (Samson 1967) may substantially reduce this kind of error.

Due to the effects discussed above small changes in the shape of the relative excitation function may arise. A calculation reveals that when all three of these errors of a geometrical origin work in one direction a maximum systematic error of 2·5% in the relative excitation cross sections may be present at 2000 eV (compared to the case of unpolarised radiation). Taking the RMS of the three contributions discussed then the systematic error is only 1·5%. In the derivation of these error limits it was supposed that only one of the extreme outer regions of the grating is effectively used and the rest of the grating is ineffective. Furthermore for both grating and multiplier extreme sensitivity for the degree of polarisation of the radiation was assumed. For the polarisation degree of the radiation emitted at 55° to the electron beam a value of -17% was used when the ^{1}P levels were excited by 2000 eV electrons. This result

was found with the help of the Bethe approximation (McFarlane 1974) and equation (6).

The most critical parameter obtained from a straight-line fit to the points in a Fano plot is ln c_n (equation (11)). Even small changes in the shape of the excitation function result in considerable changes in ln c_n. We assume the radiation to be unpolarised (so there is no influence of the effects discussed) when the excitation takes place by 300 eV electrons. For the case of a systematic error of 1·5% at 2000 eV we find a systematic error of about 4·5% in the value obtained for ln c_n (see table 1). The slope of the fit and consequently the normalisation factor would be in error by about 4%.

7. Results and discussion

7.1. Total excitation cross sections

Good quality fits (as measured by the χ^2 probability) to the Fano plots of the data on the 2^1P and 3^1P levels obtained at 55° to the electron beam were found by using measurements in the energy range of 350–2000 eV. Dropping more measurements on the low-energy side did not result in a further lowering of the χ^2 values, but considerably enhanced the statistical errors in the values found for ln c_n.

The results of de Jongh and van Eck (1971) (measured with a different type of spectrometer to the present one) revealed a similar behaviour when a weighted least-squares fit was made to their Fano plots and χ^2 tests were performed (see table 1). These results are consistent with the results of Dillon and Lassettre (1975) (see table 2), but not with the results of Donaldson *et al* (1972). In the work of Donaldson *et al* (1972) fits were used through points between 500 eV and 2000 eV but their measuring points exhibit the straight-line behaviour down to much lower energies, even as low as 200 eV.

The ln c_n values acquired from the fits are given in table 1. The error limits given for the present case include only those due to statistics. The maximum possible error of a systematic origin (§ 6) may exceed those due to statistics. The results of Donaldson *et al* (1972) differ somewhat from the present and those of de Jongh and van Eck (1971) but

Table 1. Values of the constant ln c_n appearing in equation (11) as found from a least-squares fit to the experimental data in a Fano plot. The range of energies included in the determination of the fits are listed separately in brackets. The error limits stated only concern statistical errors.

	2^1P	3^1P
Present work (weighted least-squares fit with χ^2 test)	−1·98±0·05 (350–2000 eV)	−1·87±0·07 (350–2000 eV)
de Jongh (1971) (unweighted least-squares fit)	−1·90±0·14 (200–2000 eV)	−1·90±0·14 (200–2000 eV)
Our recalculation of de Jongh (1971) (weighted least-squares fit with χ^2 test)	−1·95±0·07 (400–2000 eV)	−1·88±0·10 (300–2000 eV)
Donaldson *et al* (1972) (unweighted least-squares fit)	−2·09±0·15 (500–2000 eV)	−1·69±0·15 (500–2000 eV)
Kim and Inokuti (1968) (accurate calculation using Hylleraas-type wavefunctions)	−1·87	−1·83

there seems no reason to conclude there is an inconsistency between the calculated values of Kim and Inokuti (1968) and the experimental results (although the theoretical results are on the whole lower than the experimental results). In the region $E \geqslant 350$ eV our results for the total excitation cross sections may be found to within 2% using equation (11) and the $\ln c_n$ values given in table 1 with $f_2 = 0{\cdot}276$ and $f_3 = 0{\cdot}0734$, respectively.

In figure 6 the ratio of cross sections for excitation of the 2^1P and 3^1P levels (corrected for cascade) is given for several energies. Again our results are in good agreement with those of de Jongh and van Eck (1971). Figure 6 shows that this ratio is predicted quite well by the Born approximation for energies as low as 100 eV. The ratios of Donaldson *et al* (1972) differ by 8 to 15% from the present results but confirm the rise of this ratio in the range of lower energies ($E < 100$ eV).

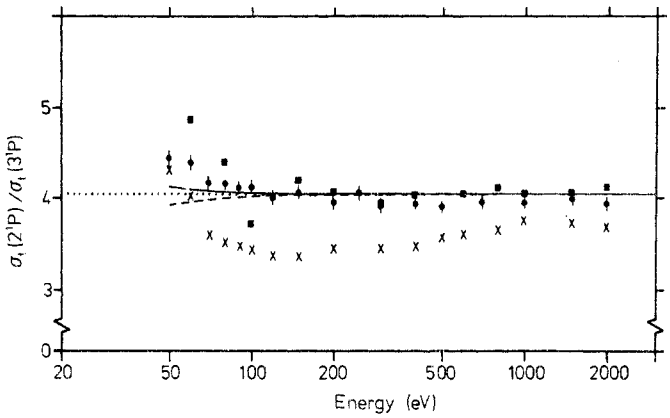

Figure 6. Ratio of total cross sections for excitation of the 2^1P and 3^1P helium levels (corrected for cascade) as a function of electron energy. ●, present results; ■, de Jongh and van Eck 1971; ×, Donaldson *et al* 1972; - - -, Kim and Inokuti 1968 (Bethe approximation); ———, Bell *et al* (1969) (Born approximation).

In tables 2 and 3 total cross sections are given for excitation of the 2^1P and 3^1P levels, respectively, in the lower energy range. Both experimental and theoretical results of several authors are included for comparison. Where possible we have given excitation cross sections *including* cascade when obtained from photon spectral intensities (to make a comparison more meaningful). Estimated cascade corrections which should be applied are listed separately (columns (*a*) of tables 2 and 3). The cascade corrections were taken from de Jongh (1971) and from Donaldson *et al* (1972) by taking mean values and partly by interpolation. (The corrections given by these authors are in good agreement with each other. The differences hardly exceed 10% of the values given here for the cascade corrections.) The statistical errors in the present results (as found from experiment) are smaller than 2%.

Results of some recent investigations (cascade corrected) together with theoretical results are shown in figures 7 and 8. Most recent calculations improve upon the Born approximation (Bell *et al* 1969) when $E \geqslant 150$ eV. However, only two of them show satisfactory agreement for the lower energies, i.e. the first-order many-body approach of Thomas *et al* (1974) and the distorted-wave polarised-orbital method of Scott and

Table 2. Comparison of total cross sections for excitation of the 2^1P state of helium (10^{-23} m^2).
Experiments

		Including cascade							
E(eV)	(*a*)	(*b*)	(*c*)	(*d*)	(*e*)	(*f*)	(*g*)	(*h*)	(*i*)
25		32·0							
28		43·2							
30	12·0	49·5		49·9					
32	12·2	56·5							
35	12·5	66·8							
40	12·7	77·0	81·8	82·4					
45	12·0	89·0							
50	11·3	93·3	97·0	97·8	97·5				
60	10·2	105·4	114·4	105·8	108				86
70	9·5	107·2		109·8					
80	8·9	110·4	108·1	111·6	98·7				93
90	8·6	110·1		111·7					
100	8·2	109·2	109·0	110·4	87·0	123·2	87		
120	7·1	103·4	111·0	105·6					
150	6·0	97·8	101·3	98·3	81·0	104·7			
180	5·4	93·5							
200	4·8	87·8	91·2	86·6	71·0	91·5	76	86·8	
250	4·1	80·4	84·1	76·5	64·0				
300	3·5	73·0	77·2	68·5	57·9	72·3	65	71·7	
350	3·1	67·2							
400	2·6	62·0	62·9	57·8	50·4	60·3	55	61·1	
500	2·2	52·9	54·1	50·7	44·4			52·9	
1000	1·1	32·5	32·9	31·3	28·9				
1500	0·7	24·1	24·2	23·5	21·0				
2000	0·6	19·1	19·6	18·7	16·9				

(*a*) Cascade corrections to be applied to columns (*b*)–(*d*).
(*b*) Present results (XUV radiation; including cascade).
(*c*) de Jongh (1971) (XUV radiation; his cascade corrections added).
(*d*) Donaldson *et al* (1972) (XUV radiation; their cascade corrections added).
(*e*) Moustafa Moussa *et al* (1969) (XUV radiation).
(*f*) Vriens *et al* (1968) (numerical integration of apparent generalised oscillator strengths fitted by a polynomial).
(*g*) Chamberlain *et al* (1970) (renormalisation of *f*).
(*h*) Dillon and Lassettre (1975) (numerical integration of apparent generalised oscillator strengths fitted by a polynomial).
(*i*) Chutjian and Srivastava (1975) (numerical integration of differential cross sections).

McDowell (1976). In particular, the latter calculation agrees very well with the present results over the whole energy range covered by figures 7 and 8. There is only a slight overestimation of the cross sections. Improvements on the Born approximation in predicting total excitation cross sections have also been obtained with recent Glauber calculations (Chan and Chen 1974a, b, Terebey 1974, Joachain and Vanderpoorten 1974) and with the distorted-wave calculation of Madison and Shelton (1973).

The near-threshold part of the excitation function for the 2^1P state which was used in § 2 for calibration of the energy scale (figure 2) was brought on an absolute scale in previous work (Westerveld and van Eck 1975). The normalisation was performed by

Table 2. (continued)

Calculations

							(*p*)	
E(eV)	(*j*)	(*k*)	(*l*)	(*m*)	(*n*)	(*o*)	I	II
25								
28								
30					31·2†			
32								
35								
40					72·5†	103·6	79·2	68·1
45								
50		149·0	189·1	170·8		114·7	102·6	90·3
60					100·8†	120·1		
70								
80					110·3†	120·3	120·3	109·1
90								
100	128·1	130·6	136·4	127·9		115·4	117·3	107·3
120								
150	108·3	109·4				101·7	102·6	95·1
180								
200	93·4	94·0	92·4	88·3		89·8	89·3	83·3
250	82·3							
300	73·7	74·0	72·3			72·1	70·8	66·6
350	66·9							
400	61·4	61·5	59·9	57·6		60·1		
500	52·9	53·0	51·1			51·5		
1000	32·3	32·3	31·8	30·9				
1500	23·8							
2000	19·1	19·1						

† The energy values as given by the authors have been rounded off to integer numbers.
(*j*) Kim and Inokuti (1968) (Bethe approximation).
(*k*) Bell *et al* (1969) (Born approximation).
(*l*) Berrington *et al* (1973) (second-order potential, impact-parameter treatment).
(*m*) Baye and Heenen (1974) (second-order diagonalisation).
(*n*) Thomas *et al* (1974) (first-order many-body calculation).
(*o*) Flannery and McCann (1975) (ten-channel eikonal approximation).
(*p*) Scott and McDowell (1976) (distorted-wave polarised-orbital DWPO I and II).

comparing the count rate at 25 eV with the count rate at higher energies (100–250 eV). For the sake of completeness this result is mentioned here to demonstrate the reasonable agreement with the calculation of Oberoi and Nesbet (1973).

7.2. Cross sections for excitation of the magnetic sublevels

In figure 9 Fano plots are given for the sublevel cross sections obtained as outlined in § 4 (cascade corrections were treated as unpolarised). Theoretical excitation cross sections for the sublevels were obtained in the Born approximation by combining the total

Table 3. Comparison of total cross sections for excitation of the 3^1P state of helium ($10^{-23}m^2$).
Experiments

		Including cascade						
E(eV)	(*a*)	(*b*)	(*c*)	(*d*)	(*e*)	(*f*)	(*g*)	(*h*)
25		5·4						
28		7·6						
30	1·8	9·2		9·6			9·0	
32	1·9	11·4						
35	1·9	13·0					13·1	
40	1·9	15·7	15·3	17·0			16·8	
45	1·9	18·5					19·9	
50	1·8	20·2	17·8	21·7		20·5	22·4	
60	1·6	23·2	23·0	25·3		22·8	26·0	
70	1·5	24·9		29·3			28·2	
80	1·4	25·7	23·9	30·6		24·7	29·2	22·0
90	1·3	25·8		30·9			29·8	
100	1·2	25·6	27·2	30·9	26·2	26·0	30·0	28·0
120	1·0	25·1		30·3				
150	0·9	23·5	23·7	28·4		23·8	27·8	
180	0·9	22·9						
200	0·8	21·6	22·1	24·5	20·1	21·1	25·3	
250	0·7	19·5	19·9	21·6		19·4		
300	0·6	18·3	18·2	19·4	17·5	17·0	20·4	
350	0·5	16·8				15·7		
400	0·4	15·5	15·5	16·3		14·0	16·8	
500	0·4	13·3	13·3	13·9	13·0	12·1	14·4	
1000	0·2	8·13	8·06	8·51		7·34	8·71	
1500	0·1	5·98	6·03	6·24		5·34		
2000	0·1	4·78	4·62	5·01		4·32		

(*a*) Cascade corrections to be applied to columns (*b*)–(*e*).
(*b*) Present results (XUV radiation; including cascade).
(*c*) de Jongh (1971) (XUV radiation; his cascade corrections added).
(*d*) Donaldson *et al* (1972) (XUV radiation; their cascade corrections added).
(*e*) Showalter and Kay (1975) (visible radiation $3^1P \rightarrow 2^1S$; including cascade).
(*f*) Moustafa Moussa *et al* (1969) (visible radiation $3^1P \rightarrow 2^1S$).
(*g*) van Raan *et al* (1971) (visible radiation $3^1P \rightarrow 2^1S$).
(*h*) Chutjian (1976) (numerical integration of differential cross sections).

excitation cross sections of Bell *et al* (1969) with the polarisation fractions of Vriens and Carrière (1970).

For the $m = 0$ sublevels the optically forbidden character of the excitation is clearly demonstrated. The Bethe approximation is not in accordance with experiment in this case until energies larger than 500 eV are reached, but the Born approximation gives considerably better agreement. This is in contrast with the optically allowed excitation process for the $m = \pm 1$ sublevels where the Bethe approximation is in even better agreement with experiment than the Born approximation for energies as low as 100 eV. Figure 9 might suggest some structure in the excitation function of the $m = 0$ sublevel in the energy range from 250 to 500 eV. Therefore a separate measurement was made in the visible region of the spectrum on the transition $3^1P \rightarrow 2^1S$. The

Table 3. (continued)

Calculations

							(*o*)	
E(eV)	(*i*)	(*j*)	(*k*)	(*l*)	(*m*)	(*n*)	I	II
25								
28								
30					5·5†			
32								
35								
40					17·0†	23·6	16·3	13·8
45								
50		36·1		45·3		26·7	23·2	20·2
60						28·5		
70								
80						28·5	29·2	26·3
90								
100	32·1	32·2	35·4	33·7		27·9	28·9	26·3
120								
150	27·0	27·1				24·7	25·7	23·7
180								
200	23·2	23·3	23·7	22·7		22·0	22·4	20·9
250	20·4							
300	18·3	18·3	18·1			17·8	17·9	16·7
350	17·4							
400	15·2	15·2	14·9	14·4		15·0		
500	13·1	13·1	12·4			12·8		
1000	7·98	7·98	7·68	7·63				
1500	5·88	5·88						
2000	4·71	4·71						

† The energy values as given by the authors have been rounded off to integer numbers.
(*i*) Kim and Inokuti (1968) (Bethe approximation).
(*j*) Bell *et al* (1969) (Born approximation).
(*k*) Bransden and Issa (1975) (second-order potential, impact-parameter treatment).
(*l*) Baye and Heenen (1974) (second-order diagonalisation).
(*m*) Chutjian and Thomas (1975) (first-order many-body calculation).
(*n*) Flannery and McCann (1975) (ten-channel eikonal approximation).
(*o*) Scott and McDowell (1976) (distorted-wave polarised-orbital DWPO I and II).

contributions to the radiation intensity originating from the $m = 0$ and $m = \pm 1$ sublevels, respectively, were separated with the help of a polariser. (The direction of observation was at right angles to the electron beam.) A multichannel analyser was used to record the polarised intensities directly by sweeping the incident energy from 250–550 eV synchronously with the channel number. The intensities appeared as smoothly varying functions without any structure (see the extreme right-hand side of figure 9).

In the low-energy region we give our results in the form of polarisation fractions (figure 10). Considering the fact that only statistical errors have been taken into account the error bars are substantial. No corrections for cascade have been applied in this energy region. Also shown are the measurements of Mumma *et al* (1974) and of

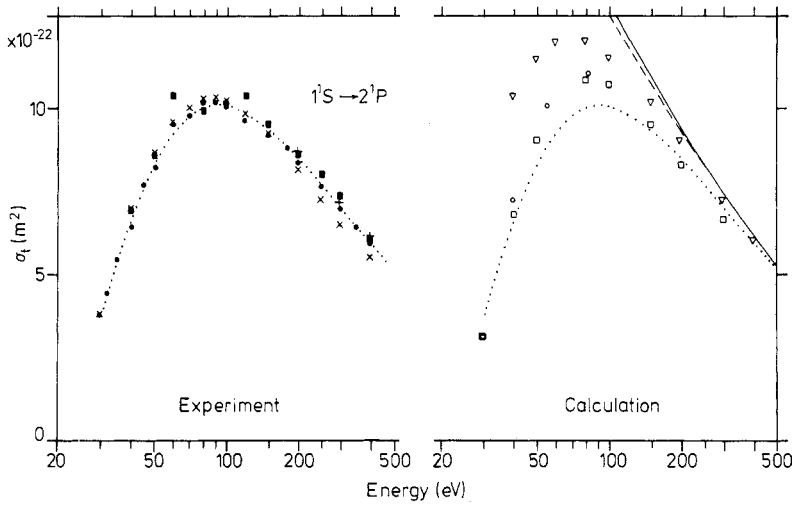

Figure 7. Total cross sections for excitation of the 2^1P helium level (corrected for cascade) by electrons in the energy range 30–400 eV. *Experiment*: ●, present work; ■, de Jongh and van Eck (1971); ×, Donaldson *et al* (1972); +, Dillon and Lassettre (1975). *Calculations*: - - -, Kim and Inokuti (1968) (Bethe approximation); ———, Bell *et al* (1969) (Born approximation); ○, Thomas *et al* (1974) (first-order many-body theory); ▽, Flannery and McCann (1975) (ten-channel eikonal treatment); □, Scott and McDowell (1976) (distorted-wave polarised-orbital method DWPO II). The dotted curves merely serve as guides to the eye to facilitate a comparison of the two parts of the figure.

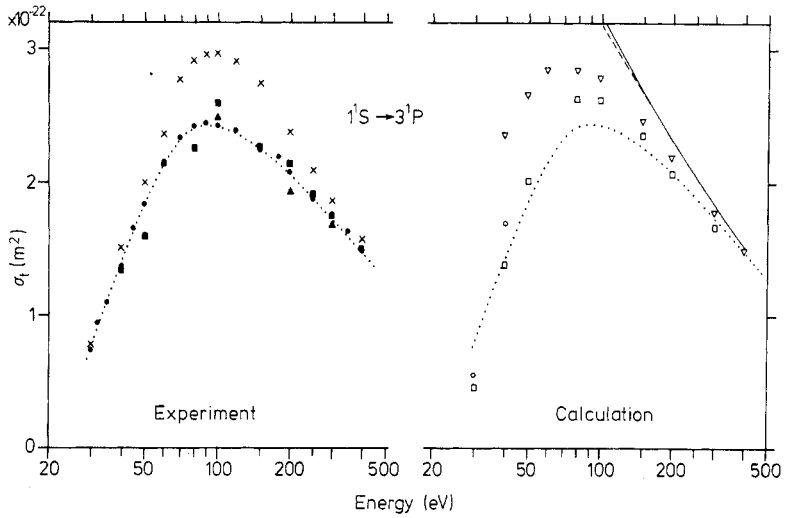

Figure 8. As figure 7, but for 3^1P. *Experiment*: ▲, Showalter and Kay (1975). *Calculations*: ○, Chutjian and Thomas (1975) (first-order many-body theory).

Heddle and Lucas (1963). In the work of Mumma *et al* (1974) the anisotropy of the total XUV emission was measured whereas Heddle and Lucas (1963) measured the degree of polarisation of the $3^1P \rightarrow 2^1S$ radiation. Recently Standage (1977) obtained polarisation fractions for excitation of the 2^1P and 3^1P states by integrating results of electron–photon coincidence experiments over the directions of the observed scattered

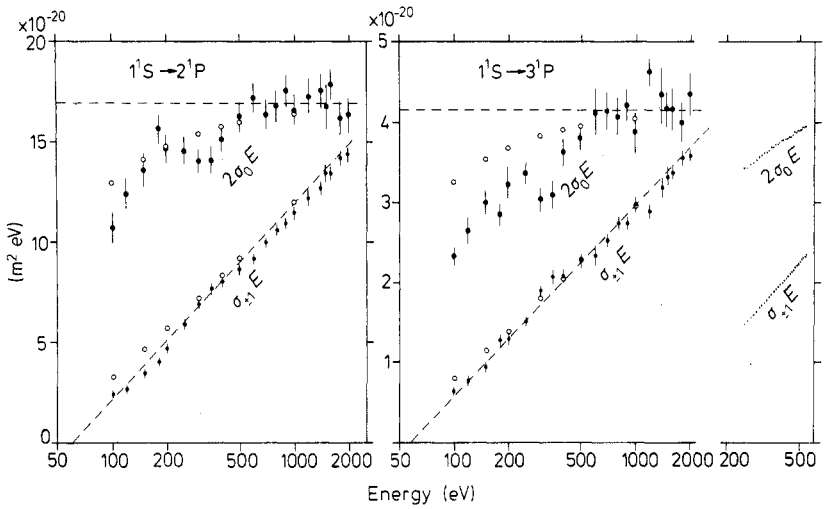

Figure 9. Fano plots of the cross sections for excitation of the magnetic sublevels of the 2^1P and 3^1P states of helium. The cross sections were obtained by combining the results of measurements at 55° and 90° to the incident electron beam (figures 4 and 5). The broken lines represent the Bethe approximation obtained using the calculations of Kim and Inokuti (1968) and equations (12) and (13). Born approximation results (○) were obtained using the calculations of Bell *et al* (1969) and of Vriens and Carrière (1970). The extreme right-hand part of the figure concerns the excitation of the 3^1P level, measured via the transition $3^1P \rightarrow 2^1S$ in the visible region of the spectrum. Here a polariser was used to record separately the contributions of the $m = 0$ and $m = \pm 1$ sublevels.

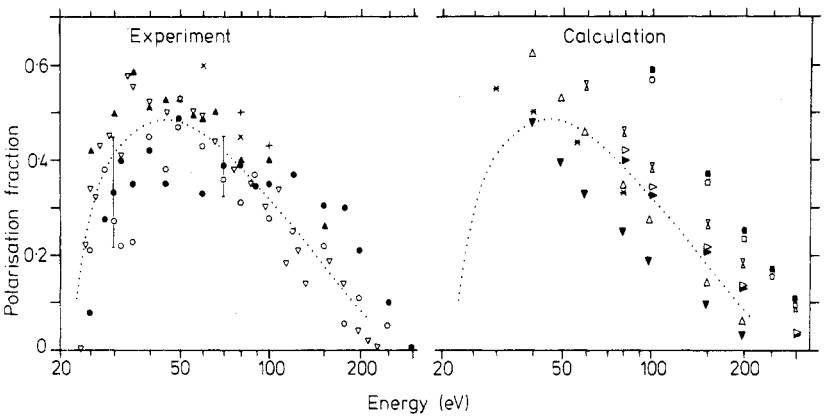

Figure 10. Polarisation fractions for radiative transitions from the electron beam excited 2^1P and 3^1P levels to ^1S levels as a function of electron energy (including cascade except where stated otherwise). *Experiment*: ●, ○, present work ($2^1P, 3^1P \rightarrow 1^1S$); ▲, Mumma *et al* (1974) ($\Sigma n^1P \rightarrow 1^1S$); ▽, Heddle and Lucas (1963) ($3^1P \rightarrow 2^1S$); ×, Standage (1977) ($2^1P \rightarrow 1^1S$, without cascade); +, Standage (1977) ($3^1P \rightarrow 1^1S$, 2^1S, without cascade). *Calculations* (no cascade included): ■, □, Bethe approximation, McFarlane (1974) (2^1P, 3^1P); ►, ▷, Born approximation, Vriens and Carrière (1970) (2^1P, 3^1P); ▼, △, ten-channel eikonal treatment, Flannery and McCann (1975) (2^1P, 3^1P); *, first-order many-body theory, Thomas *et al* (1974) (2^1P); ⧖, Glauber approximation, Chan and Chen (1974b) (3^1P). The dotted curves merely serve as guides to the eye to facilitate a comparison of the two parts of the figure.

electrons. In these electron–photon coincidence measurements the levels concerned are isolated by selection of the scattered electrons. Therefore the results are free from contributions of cascade.

In view of the large uncertainties there is reasonable agreement between the present results and those of Mumma *et al* (1974) and of Heddle and Lucas (1963), although the present results are somewhat lower in the energy range from near threshold to 100 eV. There has been some controversy concerning the polarisation fractions reported by van Eck and de Jongh (1970) (van Raan *et al* 1971) and by Moustafa Moussa *et al* (1969). A comparison of the papers of van Eck and de Jongh (1970) and of van Raan *et al* (1971) seems to indicate that in these works the pressures used were too high so that depolarisation by imprisonment of resonance radiation may have taken place (see Perel and Fedorov 1966).

Just as for the ratio of the total cross sections for excitation of 2^1P and 3^1P states, respectively, the Born approximation (Vriens and Carrière 1970) seems to work well, even for quite low energies, in predicting polarisation fractions, as was noticed previously by Mumma *et al* (1974). Here the Bethe theory fails entirely as we recognised before in the range of energies from 100 to 400 eV (figure 9). Surprisingly the results of more advanced calculations improve, at best, only marginally upon the Born approximation. Possible exceptions may be the distorted-wave treatments by Madison and Shelton (1973) and Scott and McDowell (1976). Their calculated λ parameters appear to agree quite well with those obtained from electron–photon coincidence experiments (the λ parameter at an electron scattering angle θ is defined as the ratio of the differential cross section for excitation of the $m = 0$ sublevel and the differential cross section summed over the sublevels). For further details see Kleinpoppen *et al* (1975), Scott and McDowell (1976) and Sutcliffe *et al* (1978).

In conclusion we may state that the measurement and the calculation of total cross sections for excitation of ^1P helium levels has greatly progressed in the last few years. The polarisation fractions, however, need further attention both experimentally and theoretically.

Acknowledgments

We gratefully acknowledge stimulating discussions with Professor J A Smit. This work was performed as part of the research programme of the 'Stichting Fundamenteel Onderzoek der Materie' (FOM) with financial support from the 'Nederlandse Organisatie voor Zuiver Wetenschappelijk Onderzoek' (ZWO).

References

Baye D and Heenen P H 1974 *J. Phys. B: Atom. Molec. Phys.* **7** 938–49
Bell K L, Kennedy D J and Kingston A E 1969 *J. Phys. B: Atom. Molec. Phys.* **2** 26–43
Berrington K A, Bransden B H and Coleman J P 1973 *J. Phys. B: Atom. Molec. Phys.* **6** 436–49
Bransden B H and Issa M R 1975 *J. Phys. B: Atom. Molec. Phys.* **8** 1088–94
Brunt J N H, King G C and Read F H 1977 *J. Electron Spectrosc. Rel. Phen.* **12** 221–8
Chamberlain G E and Heideman H G M 1965 *Phys. Rev. Lett.* **15** 337–8
Chamberlain G E, Mielczarek S R and Kuyatt C E 1970 *Phys. Rev.* A **2** 1905–22
Chan F T and Chen S T 1974a *Phys. Rev.* A **9** 2393–7
—— 1974b *Phys. Rev.* A **10** 1151–6

Chutjian A 1976 *J. Phys. B: Atom. Molec. Phys.* **9** 1749–56
Chutjian A and Srivastava S K 1975 *J. Phys. B: Atom. Molec. Phys.* **8** 2360–8
Chutjian A and Thomas L D 1975 *Phys. Rev.* A **11** 1583–95
Clout P N and Heddle D W O 1969 *J. Opt. Soc. Am.* **59** 715–7
de Jongh J P 1971 *Thesis* University of Utrecht
de Jongh J P and van Eck J 1971 *Proc. 7th Int. Conf. on Physics of Electronic and Atomic Collisions, Amsterdam* (Amsterdam: North Holland) Abstracts pp 701–3
Dillon M A and Lassettre E N 1975 *J. Chem. Phys.* **62** 2373–90
Donaldson F G, Hender M A and McConkey J W 1972 *J. Phys. B: Atom. Molec. Phys.* **5** 1192–210
Eminyan M, MacAdam K B, Slevin J and Kleinpoppen H 1974 *J. Phys. B: Atom. Molec. Phys.* **7** 1519–42
Flannery M R and McCann K J 1975 *J. Phys. B: Atom. Molec. Phys.* **8** 1716–33
Heddle D W O and Lucas C B 1963 *Phil. Trans. R. Soc.* A **271** 129–42
Hunter W R 1974 *Proc. 4th Int. Conf. on Vacuum Ultra-Violet Radiation Physics, Hamburg* (Braunschweig: Vieweg) pp 683–707
Inokuti M 1971 *Rev. Mod. Phys.* **43** 297–347
Joachain C J and Vanderpoorten R 1974 *J. Phys. B: Atom. Molec. Phys.* **7** 817–30
Kim Y K and Inokuti M 1968 *Phys. Rev.* **175** 176–88
Kleinpoppen H, Blum K and Standage M C 1975 *Proc. 9th Int. Conf. on Physics of Electronics and Atomic Collisions, Seattle* (Seattle: University of Washington Press) *Invited Lectures and Progress Reports* pp 641–9
Lukirskii A P and Fomichev V A 1965 *Opt. Spectrosc.* **19** 441–5 (1965 *Opt. Spektrosk.* **19** 800–8)
McFarlane S C 1974 *J. Phys. B: Atom. Molec. Phys.* **7** 1756–71
Macek J and Jaecks D H 1971 *Phys. Rev.* A **4** 2288–300
Madison D H and Shelton W N 1973 *Phys. Rev.* A **7** 499–513
Mathews J and Walker R L 1970 *Mathematical Methods of Physics* 2nd edn (New York: Benjamin) pp 387–401
Mentall J E and Morgan H D 1976 *Phys. Rev.* A **14** 954–60
Moustafa Moussa H R 1967 *Thesis* University of Leiden
Moustafa Moussa H R, de Heer F J and Schutten J 1969 *Physica* **40** 517–49
Mumma M J, Misakian M, Jackson W M and Faris J L 1974 *Phys. Rev.* A **9** 203–8
Oberoi R S and Nesbet R K 1973 *Phys. Rev.* A **8** 2969–79
Perel V I and Fedorov V L 1966 *Opt. Spectrosc.* **20** 417–20 (1966 *Opt. Spectrosk.* **20** 745–9)
Samson J A R 1967 *Techniques of Vacuum Ultraviolet Spectroscopy* (New York: Wiley) pp 25–35
Schiff B, Pekeris C L and Accad Y 1971 *Phys. Rev.* A **4** 885–93
Scott T and McDowell M R C 1976 *J. Phys. B: Atom. Molec. Phys.* **9** 2235–54
Showalter J G and Kay R B 1975 *Phys. Rev.* A **11** 1899–910
Standage M C 1977 *J. Phys. B: Atom. Molec. Phys.* **10** 2789–96
Sutcliffe V C, Hadad G N, Steph N C and Golden D E 1978 *Phys. Rev.* A **17** 100–7
Terebey J Z 1974 *J. Phys. B: Atom. Molec. Phys.* **7** 460–7
Thomas L D, Csanak G, Taylor H S and Yarlagadda B S 1974 *J. Phys. B: Atom. Molec. Phys.* **7** 1719–33
Tomaš M S, Lucas A A, Šunjić M and Juretić D 1974 *Phys. Rev.* B **4** 1489–98
van Eck J and de Jongh J P 1970 *Physica* **47** 141–58
van Raan A F J, de Jongh J P, van Eck J and Heideman H G M 1971 *Physica* **53** 45–59
Vriens L and Carrière J D 1970 *Physica* **49** 517–31
Vriens L, Simpson J A and Mielczarek S R 1968 *Phys. Rev.* **165** 7–15
Westerveld W B and van Eck J 1975 *Proc. 9th Int. Conf. on Physics of Electronic and Atomic Collisions, Seattle* (Seattle: University of Washington Press) Abstracts pp 782–3
Westerveld W B and van Eck J 1977 *J. Quant. Spectrosc. Radiat. Transfer* **17** 131–8